analytical chemistry

Article

pubs.acs.org/ac



# Amphipathic Polymers Enable the Study of Functional Membrane Proteins in the Gas Phase

Aneika C. Leney, Lindsay M. McMorran, Sheena E. Radford,* and Alison E. Ashcroft*

Astbury Centre for Structural Molecular Biology, School of Molecular and Cellular Biology, University of Leeds, Leeds LS2 9JT, United Kingdom

**ABSTRACT:** Membrane proteins are notoriously challenging to analyze using mass spectrometry (MS) because of their insolubility in aqueous solution. Current MS methods for studying intact membrane proteins involve solubilization in detergent. However, detergents can destabilize proteins, leading to protein unfolding and aggregation, or resulting in inactive entities. Amphipathic polymers, termed amphipols, can be used as a substitute for detergents and have been shown to enhance the stability of membrane proteins. Here, we show the utility of amphipols for investigating the structural and functional properties of membrane proteins using electrospray ionization mass spectrometry (ESI-MS). The functional properties of two bacterial outer-membrane $\beta$-barrel proteins, OmpT and PagP, in complex with the amphipol A8-35 are demonstrated, and their structural integrities are confirmed in the gas phase using ESI-MS coupled with ion mobility spectrometry (IMS). The data illustrate the power of ESI-IMS-MS in separating distinct populations of amphipathic polymers from the amphipol−membrane complex while maintaining a conformationally "nativelike" membrane protein structure in the gas phase. Together, the data indicate the potential importance and utility of amphipols for the analysis of membrane proteins using MS.

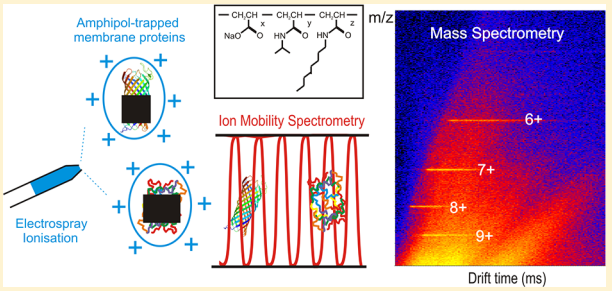


Integral membrane proteins play essential roles in many biological processes, such as transport of solutes, signaling, and energy transduction. Despite this, our fundamental knowledge of the structure of membrane proteins and how they fold, assemble, and function remains limited. Membrane proteins are notoriously difficult to study; their expression and purification is challenging, and problems occur when trying to preserve the structural activity and the stability of these proteins in vitro.[1]

Currently the most common method to study membrane proteins in aqueous solution involves the initial solubilization of the protein in micelle-forming detergent molecules. However, detergent micelles are not optimal for preserving membrane protein function due to their highly dynamic nature, and thus, protein unfolding and aggregation in detergent micelles are commonly observed.[2,3] In addition, the spherical micelles do not always provide a nativelike environment for the proteins, poorly mimicking the physical and chemical properties of the planar cellular membrane depending on the match of the detergent and the lipid. Therefore, alternative membrane solubilization techniques are needed.[1,4]

One alternative to exploiting detergent micelles for membrane protein solubilization are amphipathic polymers termed amphipols that were designed to bind noncovalently to the transmembrane region of membrane proteins in a quasi-irreversible manner.[4,5] The major benefit of amphipols is that they can allow membrane proteins to fold into their native state in detergent-free solution. Additionally, membrane proteins complexed with amphipols have an increased stability compared with those in detergent.[4,5] Over the past few years, amphipols have been used to study membrane protein complexes using a variety of biochemical techniques including size-exclusion chromatography,[6] electron microscopy,[7] analytical ultracentrifugation,[6] fluorescence resonance energy transfer,[8] and solution NMR.[9−11] A recent publication described the use of matrix-assisted laser desorption ionization mass spectrometry (MALDI-MS) to determine the molecular mass of the amphipol-trapped membrane proteins bacteriorhodopsin, OmpA, cytochrome $b_6f$, and cytochrome $bc_1$.[12] However, the conformational properties of the membrane proteins in the gas phase cannot be determined using this approach, and their functional behavior cannot be studied.

Here, we demonstrate the application of electrospray ionization mass spectrometry (ESI-MS), and ESI-MS coupled with ion mobility spectrometry (IMS), to the study of native membrane proteins in complex with amphipols. Two bacterial $\beta$-barrel outer-membrane proteins (PagP and OmpT), whose interactions with amphipols have not previously been studied, were folded into the amphipol, A8-35 (Figure 1A). In both cases, the proteins were highly stable, remaining functionally active for several months in complex with the amphipol at 4 °C in ammonium hydrogen carbonate, pH 8. ESI-IMS-MS enabled separation of the amphipol from the membrane proteins in the gas phase, thus allowing the conformational properties of both

**Received:** August 3, 2012
**Accepted:** October 16, 2012
**Published:** October 16, 2012

  

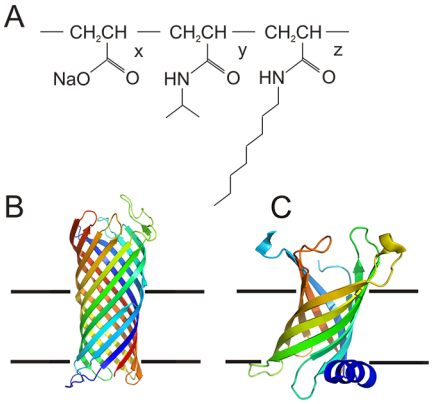


**Figure 1.** (A) Amphipol A8-35 of molecular weight 9−10 kDa; $x$ = 29−34%; $y$ = 25−28%; and $z$ = 39−44%. Crystal structures of the membrane proteins (B) OmpT (PDB file 1I78)[34] and (C) PagP (PDB file 1THQ).[35].

OmpT and PagP within the membrane protein−amphipol complex to be determined. The results highlight the power of amphipols to solubilize and maintain membrane proteins in their native state and present the first example of the analysis of the structure of membrane proteins by ESI-IMS-MS as a result of the ability of amphipols to protect and preserve membrane protein structure on transition into the gas phase.

## EXPERIMENTAL SECTION

**Sample Preparation.** $PagP_{his}$ was expressed and purified as described previously.[13] The gene encoding the mature OmpT sequence was amplified from *Escherichia coli* XL1-blue cells using polymerase chain reaction (PCR), ligated into the pET-11a plasmid vector using *Bam*HI and *Nde*I restriction sites, and transformed into BL21 (DE3) *E. coli* cells to enable protein overexpression. Overexpression and subsequent isolation of inclusion bodies of OmpT were carried out as described by Burgess et al.[14] To purify the protein further, OmpT inclusion bodies were gel-filtered in 6 M guanidine hydrochloride using a Superdex 75 HiLoad 26/60 column (GE Healthcare, Little Chalfont, Bucks, U.K.). Inclusion bodies were solubilized in 6 M guanidine hydrochloride, 25 mM Tris−HCl, pH 8.0, followed by centrifugation at 20 000$g$ for 20 min at 4 °C. The resulting supernatant was filtered through a 0.2 $\mu$M syringe filter before loading onto the column. Following gel filtration, OmpT was precipitated by dialysis against deionized $H_2O$, and the protein was stored as a precipitate at −80 °C. To fold the membrane proteins into amphipol, PagP and OmpT were dissolved initially in 100 mM ammonium hydrogen carbonate pH 8.0 containing 8 M urea. A8-35 (purchased from Affymetrix Ltd., High Wycombe, Bucks, U.K.) was then added at a protein/A8-35 ratio of 1:5 (w/w), and the resulting solution was dialyzed into 100 mM ammonium hydrogen carbonate pH 8.0 at 4 °C for 24 h. A final membrane protein concentration of 1 mg $mL^{-1}$ was used for all experiments.

**Circular Dichroism.** Far-UV circular dichroism (CD) spectra of all proteins were recorded on a Chirascan CD spectrometer (Applied Photophysics, Leatherhead, Surrey, U.K.) using a 0.1 mm path length cuvette. Eight scans were acquired over the range 200−260 nm with a bandwidth of 1.0 nm and a scan speed of 20 nm $min^{-1}$ and then averaged. Background spectra containing the amphipol and buffer alone were subtracted for all samples. The recorded CD spectra were normalized to obtain the mean residue molar ellipticity $[\Theta]$ $(\lambda)$, in deg $cm^2$ $dmol^{-1}$:

$$[\Theta](\lambda) = 100\frac{\Theta(\lambda)}{c \cdot n \cdot l}$$

where $l$ is the path length of the cuvette (cm), $\Theta(\lambda)$ is the recorded ellipticity (deg), $c$ is the concentration (moles $L^{-1}$), and $n$ is the number of amino acid residues: 297 for OmpT and 169 for PagP.

**Size-Exclusion Chromatography.** Size-exclusion chromatography (SEC) was carried out using a Superdex 200 (10/300) column connected to an Äkta Explorer system (GE Healthcare, Little Chalfont, Bucks, U.K.). A 200 $\mu$L aliquot of protein/A8-35 complex was injected onto the column pre-equilibrated in either 100 mM ammonium hydrogen carbonate pH 8.0 (folded) or 100 mM ammonium hydrogen carbonate pH 8.0 containing 8 M urea (unfolded). Elution profiles were followed using the absorbance at 280 nm for all proteins.

**Activity Assays.** To measure OmpT protease activity, the change in fluorescence emission at 430 nm of the cleavable fluorogenic peptide (Abz-Ala-Arg-Arg-Ala-Tyr-$(NO_2)$-$NH_2$) (Cambridge Peptides Ltd., Cambridge, U.K.) was measured upon excitation at 325 nm.[15] The excitation and emission slit widths were set to 2 nm, and the fluorescence was measured over a 300 s reaction time scale using a fluorimeter (Photon Technology International Inc., Ford, West Sussex, U.K.). The temperature was regulated to 25 °C using a water bath, and a 1 cm path length cuvette was used. In some experiments, lipopolysaccharide (LPS) from *E. coli* O111:B4 (cat. no. 437627, Calbiochem, Beeston, Notts, U.K.), the major component of the outer leaflet of the outer membrane in Gram-negative bacteria, was added to the OmpT−A8-35 solution at a concentration of 1 mg $mL^{-1}$. In all cases, the fluorogenic peptide was added immediately before analysis to a final concentration of 50 $\mu$M. Samples were mixed manually, resulting in a dead time of approximately 15 s. The average specific enzyme activity over a range of protein concentrations was reported as the amount of product produced per milligram of enzyme per minute; that is, the relative fluorescence units measured were expressed as a percentage of the total relative fluorescence value taken at the end of the reaction. A control in which OmpT was unfolded in 8 M urea confirmed that the observed activity resulted from the natively folded OmpT−A8-35 complex.

The enzymatic activity assay for PagP was adapted from a previously described method.[13] The hydrolysis of *p*-nitrophenyl palmitate (*p*-NPP) to *p*-nitrophenol (*p*-NP) by PagP was monitored by the increase in absorbance at 410 nm. *p*-NPP (10 mM in propan-2-ol) was diluted into 100 mM ammonium hydrogen carbonate pH 8.0 containing various concentrations of PagP/A8-35 complex to a final substrate concentration of 1 mM, and the rate of reaction was monitored over 200 min. The increase in absorbance due to A8-35 addition alone was subtracted from all measurements. A control in which PagP was unfolded in 8 M urea confirmed the activity resulted from the natively folded PagP/A8-35 complex. The average specific enzyme turnover over a range of protein concentrations was reported in nanomoles per minute per micromolar of PagP using an extinction coefficient of 3390 $M^{-1}$ $cm^{-1}$ for *p*-nitrophenol.

**Mass Spectrometry.** Experimental measurements were performed on a Synapt HDMS mass spectrometer (Micromass UK Ltd./Waters, Manchester, U.K.) equipped with a Nano-


dx.doi.org/10.1021/ac302223s | *Anal. Chem.* 2012, 84, 9841−9847

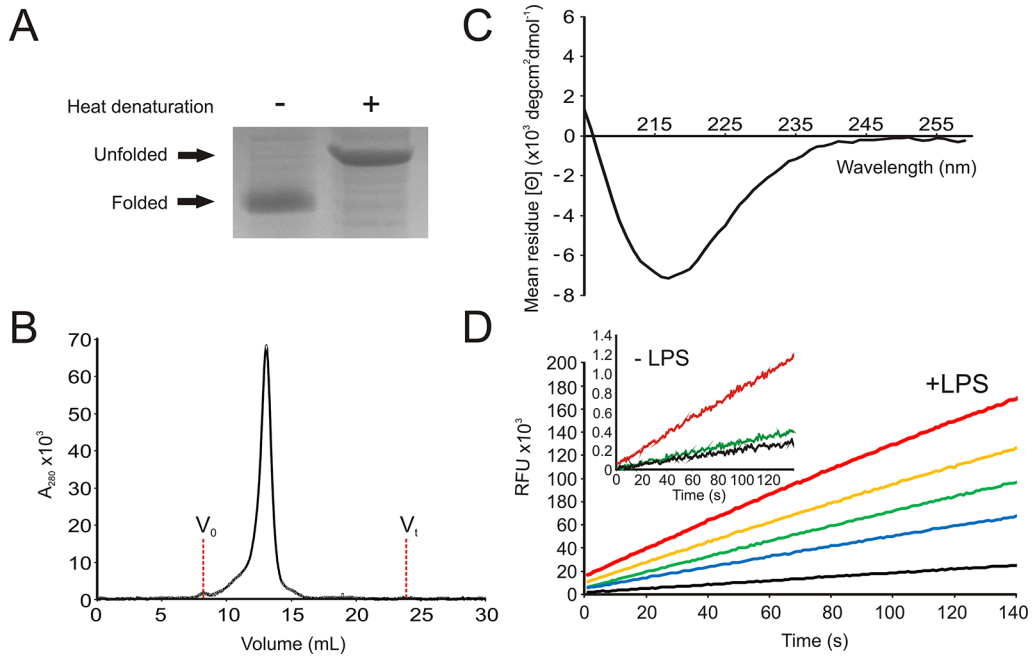


**Figure 2.** OmpT−A8-35 complex structure and function. (A) SDS-PAGE of OmpT−A8-35 complex with and without heat denaturation; (B) size-exclusion chromatogram showing a single peak corresponding to the OmpT−A8-35 complex with the void ($V_o$) and total column volumes ($V_t$) highlighted; (C) far-UV CD spectrum of the OmpT−A8-35 complex; (D) functional assay showing the fluorescence increase (relative fluorescence units) on enzymatic cleavage of the peptide Abz-Ala-Arg-Arg-Ala-Tyr-($NO_2$)-$NH_2$ on addition of 0.05 $\mu$M (black), 0.10 $\mu$M (blue), 0.15 $\mu$M (green), 0.20 $\mu$M (yellow), and 0.30 $\mu$M (red) OmpT−A8-35 complex in the presence of LPS. The inset shows the weak catalytic activity of OmpT−A8-35 without LPS at OmpT−A8-35 concentrations of 0.05 $\mu$M (black), 0.15 $\mu$M (green), and 0.30 $\mu$M (red).

Mate (Advion Biosystems Inc., Ithaca, NY, U.S.) nanoESI autosampling device. Positive nanoESI with a capillary voltage of 1.75 kV, a nitrogen nebulizing gas pressure of 0.5 p.s.i, and a source temperature of 60 °C was used throughout. For mass spectral analysis of the amphipol alone, a cone voltage of 70 V, a trap voltage of 6 V, and a transfer voltage of 4 V was applied. For analysis of PagP and OmpT in the amphipol, a cone voltage of 170 V was applied with the trap, and transfer T-wave devices were set at 150 and 100 V respectively; a backing pressure of 4.7 mbar and a trap pressure of 3.85 × $10^{-2}$ mbar were used. The bias voltage was optimized (20−150 V) in order to maximize the intensity of the membrane protein. Ion mobility separation was performed by ramping the wave height from 4.5 to 28.5 V at a speed of 300 $ms^{-1}$. Drift times were corrected for mass-dependent and mass-independent times,[16] and the drift time cross-section function was calibrated as reported previously.[17] Computer-based cross-sectional area calculations were made from Protein Data Bank structures of the two membrane proteins (Figure 1B, C) using the projection superposition approximation (PSA) method described elsewhere.[18] An aqueous solution of CsI was used for $m/z$ calibration. All data were acquired over the $m/z$ range 500−8000, and the raw data were processed by use of MassLynx v.4.1 and Driftscope v.3.0 software (Micromass UK Ltd./Waters, Manchester, U.K.).

## RESULTS AND DISCUSSION

The compatibility of amphipol−membrane protein complexes for analysis using ESI-IMS-MS was investigated through the study of two bacterial outer-membrane $\beta$-barrel proteins OmpT and PagP. The interaction between the $\beta$-barrel outer-membrane proteins OmpT and PagP with amphipols has not been reported previously.

**Folding OmpT into A8-35.** OmpT is a 10-stranded, 33.5 kDa outer-membrane $\beta$-barrel protein (Figure 1B). OmpT folds and inserts into the outer membrane of Gram-negative bacteria facilitated by the Bam complex.[19] It is only here, in the presence of lipopolysaccharide (LPS), that OmpT is functional as an outer-membrane protease.[20] To initiate folding, OmpT unfolded in 8 M urea pH 8.0, was mixed with a 5-fold excess (w/w) of the amphipol A8-35, and the resulting sample was dialyzed immediately into 100 mM ammonium hydrogen carbonate pH 8.0. OmpT remained soluble in this urea-free buffer at a concentration up to 1 mg $mL^{-1}$, and no evidence of aggregation or precipitation was apparent by use of sodium dodecyl sulfate (SDS) or mass spectrometry, suggesting that if higher order species exist, they are neither SDS-resistant nor observed in the gas phase. The stoichiometry of OmpT binding to A8-35 is unknown.

Cold sodium dodecyl sulfate polyacrylamide gel electrophoresis (SDS-PAGE) can be used to distinguish between folded and fully denatured forms of membrane proteins.[21] Indeed, when A8-35-solubilized OmpT was analyzed using cold SDS-PAGE, the protein migrated as a single band more rapidly than expected based on its molecular weight, indicating that complete refolding of OmpT had occurred into A8-35 (Figure 2A). SEC showed a single peak corresponding to the OmpT−A8-35 complex indicating that a single species is present in solution (Figure 2B). Consistent with these results, far-UV CD showed a characteristic negative maximum at 218 nm, indicating a high content of $\beta$-sheet secondary structure had formed in the OmpT−A8-35 complex (Figure 2C).

The functionality of the refolded OmpT−A8-35 complex was examined by use of a fluorescence assay. On addition of LPS, native OmpT readily cleaves an internally quenched fluorogenic peptide (Abz-Ala-Arg-Arg-Ala-Tyr-($NO_2$)-$NH_2$) resulting in an


dx.doi.org/10.1021/ac302223s | Anal. Chem. 2012, 84, 9841−9847

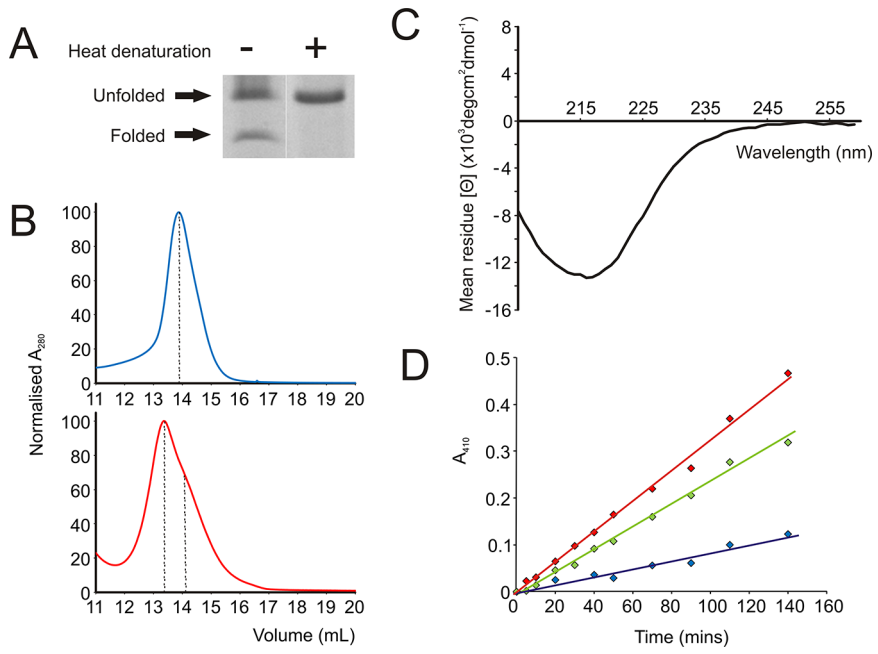


**Figure 3.** PagP−A8-35 complex structure and function. (A) SDS-PAGE of PagP−A8-35 complex with and without heat denaturation; (B) size-exclusion chromatogram showing PagP unfolded in 8 M urea (blue, top) and the PagP−A8-35 complex (red, bottom); (C) far-UV CD spectrum of the PagP−A8-35 complex; (D) functional assay showing the absorbance increase at 410 nm on hydrolysis of *p*-NPP to *p*-NP at PagP−A8-35 concentrations of 20 $\mu$M (blue), 30 $\mu$M (green), and 40 $\mu$M (red). The average specific enzyme turnover over the three protein concentrations was reported in nmol $min^{-1}$ $\mu M^{-1}$ of PagP using an extinction coefficient of 3390 $M^{-1}$ $cm^{-1}$ for *p*-nitrophenol.

increase in fluorescence at 430 nm.[15] However, in vitro experiments with OmpT in complex with detergent and liposomes have shown that no increase in fluorescence is observed in the absence of LPS.[15,22] The OmpT−A8-35 complex was incubated at various concentrations with and without LPS, and the OmpT enzyme activity was measured based on the observed increase in fluorescence of the same fluorescent peptide substrate (Figure 2D). The specific activity of OmpT was found to be 0.7 $\mu$moles of product per milligram of enzyme per minute confirming that OmpT had folded to a functional state in the amphipol. Interestingly, a small amount of activity was observed in the absence of LPS (0.1 $\mu$moles product per milligram of enzyme per minute) (Figure 2D inset). However, this is a 6-fold reduction compared with the activity observed in the presence of LPS (Figure 2D) and hence is consistent with previous results that have shown a requirement of LPS for OmpT activity.[23] Together the cold SDS-PAGE, far-UV CD, SEC, and fluorescence activity data show that OmpT folds readily into the A8-35 amphipol to form a native, functional OmpT−A8-35 complex. Interestingly, this OmpT−A8-35 complex is remarkably stable as OmpT remains folded in its $\beta$-sheet conformation, with a less than 3-fold decrease in activity over two months of storage at 4 °C.

**Folding PagP into A8-35.** The role of the smaller, 20.2 kDa membrane protein PagP (Figure 1C) is to transfer a palmitate chain from phospholipids to the lipid A moiety of LPS in the outer leaflet of the bacterial outer membrane, reinforcing the hydrocarbon core of the outer leaflet and protecting it from host immune defenses.[24] PagP was folded into A8-35 using the same procedure as described for OmpT. Cold SDS-PAGE showed that ~60% of PagP was folded into A8-35 (Figure 3A). In support of this conclusion, SEC showed a broad peak for the PagP−A8-35 complex compared with the elution profile of PagP in the urea-denatured state, also indicating a mixture of folded and unfolded PagP species to be present in solution (Figure 3A, B). Despite both the PagP/A8-35 ratio and the folding rate into the amphipol being optimized to obtain the maximum folding yield of PagP into amphipol, this was the highest yield achieved. Far-UV CD data confirmed that the PagP in complex with A8-35 has adopted a $\beta$-sheet secondary structure, with a characteristic negative maximum at 218 nm (Figure 3C). However, the positive molar ellipticity at 232 nm commonly observed in the far-UV CD spectrum of native PagP is absent.[25] The band at 232 nm arises from a Cotton effect for the interaction between residues Tyr26 and Trp66, which pack closely together in the native PagP structure.[25,26] The absence of this Cotton band likely reflects slight structural perturbations in the PagP structure in the presence of the amphipol. This has been reported previously when local structural modifications were introduced through mutation of residues in the active site of PagP.[27] However, activity assays in which the hydrolysis of *p*-nitrophenyl palmitate (*p*-NPP) to *p*-nitrophenol (*p*-NP) was monitored indicated that PagP is indeed functional in the amphipol complex (Figure 3D). The specific enzyme activity of PagP in complex with A8-35 was determined to be 0.019 ± 0.006 nmol $min^{-1}$ $\mu M^{-1}$, which is not significantly different from previous results using PagP in detergent.[13]

**ESI-IMS-MS Analysis of A8-35−Membrane Protein Complexes.** As a consequence of their heterogeneous nature, in terms of the polydispersity within their structures, the study of amphipols by mass spectrometry is challenging. Over recent years, ESI-IMS-MS has been utilized increasingly to separate polymeric mixtures allowing individual components within complex spectra to be assigned unambiguously.[28] The three-dimensional ESI-IMS-MS spectrum of the amphipol A8-35 is shown in Figure 4. Using "soft" ionization conditions, multiple species are observed from which 1+, 2+, 3+, and 4+ charge state ions can be separated clearly and identified. Under soft ionization conditions, all membrane protein−amphipol com-


dx.doi.org/10.1021/ac302223s | *Anal. Chem.* 2012, 84, 9841−9847

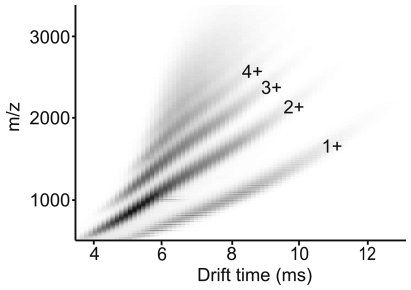


**Figure 4.** ESI-IMS-MS driftscope plot of the amphipol A8-35 alone (5 mg $mL^{-1}$ in 100 mM ammonium hydrogen carbonate, pH 8) highlighting the four different charge state ion series arising from the wide range of A8-35 polymers. The graph shows the $m/z$ of the ions vs the drift time (ms) of the ions in the IMS cell. An ion's drift time depends on both the shape (CCS) of the ion and the number of charges it carries.

plexes were undetectable by ESI-MS (data not shown), presumably because the membrane proteins remained in complex with the amphipol. However, when the settings for the trap and transfer regions of the mass spectrometer were increased to 150 and 100 V, respectively, the membrane proteins were released from the amphipol, and ions corresponding to the multiply charged membrane proteins were clearly detected (Figure 5A, B). By using ESI-IMS-MS, these ions were well separated from those arising from the amphipol. The ESI-MS spectrum of OmpT shows a narrow charge state distribution corresponding to the 6+, 7+, and 8+ ions, together with slightly more expanded 9+ ions, giving an experimentally determined mass of 33 462 ± 5 Da, which is within 0.01% of the calculated mass based on the amino acid sequence (33 460 Da).

ESI-IMS-MS was able not only to effect the release of the PagP membrane protein from the amphipol A8-35 but also to separate the folded and unfolded PagP conformers that SDS-PAGE had indicated to be present. The ESI-MS spectrum of PagP released from its complex with A8-35 shows a narrow charge distribution (5+, 6+, and 7+ charge state ions) corresponding to a compact structure of the expected molecular mass (20 175 ± 1 Da compared with 20 175 Da predicted based on the amino acid sequence), Figure 5B. However, significantly more expanded 7+ charge state ions indicative of a second conformer could also be detected in the ESI-IMS-MS driftscope plot (Figure 5B, red arrow). Higher charge states (8+, 9+, and 10+) were also observed for this more expanded PagP conformation (data not shown).

By using ESI-IMS-MS, ions are separated according to their movement through a mobility cell containing a buffer gas. By calibrating the arrival time distributions of protein ions of known structure, the collision cross-sectional areas (CCS) of unknown proteins can be estimated.[17,29] These experimental CCS values can then be compared with modeled values calculated by use of the PDB structures of the proteins of interest. If the experimentally estimated and theoretically determined CCS values are in agreement, it can be inferred that the protein retains a nativelike structure in the gas phase.[29] The experimentally estimated CCS for the lowest charge state ions of PagP and OmpT (1790 and 2601 $Å^2$, respectively) are consistent within experimental error with the values predicted from their PDB crystal structure coordinates using the projected superposition approximation method (PSA)[18] (1732 and 2718 $Å^2$, respectively). These data suggest that both PagP and OmpT remain in a nativelike conformation in the gas phase and thus demonstrate the power of amphipols in preserving membrane protein structure on transition from solution into the gas phase. An additional conformer some 70% more expanded was also observed for the membrane protein PagP (3131 $Å^2$). This observation is consistent with the SDS-PAGE and SEC data that indicate that PagP is not 100% folded in A8-35 and confirms the ability of ESI-IMS-MS to transfer and separate folded and partially folded solution structures into the gas phase.

## CONCLUSIONS

The analysis of membrane proteins by ESI-MS has been demonstrated recently following solubilization of membrane proteins in detergent micelles.[30] This approach, while very powerful, has limitations because of the instability of the membrane protein−detergent complexes and the difficulties in preserving protein structure, protein−protein, and protein−ligand interactions in detergent solutions.[1] Amphipols offer the ability to trap membrane proteins in detergent-free aqueous solutions, offering new possibilities for the structural analysis of membrane proteins by ESI-MS. Additionally, amphipols are particularly stable in aqueous solution containing low salt concentrations that are ideal conditions for mass spectral analysis.

In the present work, we have used ESI-IMS-MS to examine two different membrane proteins refolded into the amphipol A8-35. Biophysical analysis confirmed that each of the A8-35−membrane protein complexes was stable and the protein folded into a native conformation that is functionally active in the MS-compatible buffers used. ESI-IMS-MS was used to release and

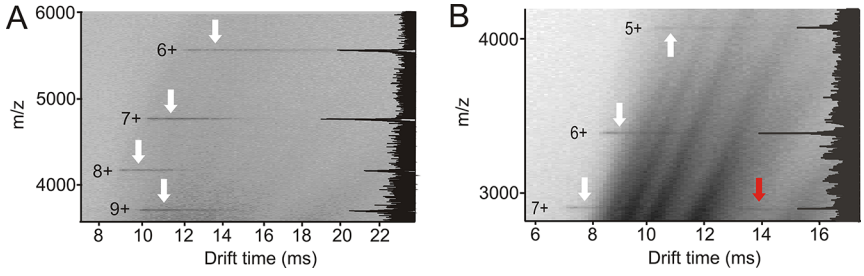


**Figure 5.** ESI-IMS-MS driftscope plots of (A) the OmpT−A8-35 complex and (B) the PagP−A8-35 complex. The charge states of the ions are labeled in all cases, and the summed $m/z$ spectrum for each complex is displayed on the right-hand side. White arrows in (A) and (B) highlight the compact protein conformer in each case, while a second, more expanded conformer is observed for the 7+ ions in the PagP−A8-35 driftscope plot (red arrow).


dx.doi.org/10.1021/ac302223s | Anal. Chem. 2012, 84, 9841−9847

separate the membrane proteins from the amphipol in the gas phase, thus allowing characterization of the membrane proteins alone. CCS calculations confirmed that A8-35 preserves these membrane proteins in a nativelike structure on transition into the gas phase, resulting in experimental CCSs within 5% of those obtained from theoretical values calculated based on the PDB structures of these proteins. Additionally, we show that ESI-IMS-MS can separate proteins populating different conformations in complex with A8-35, reflecting their solution properties. The application of A8-35 to two different $\beta$-barrel membrane proteins suggests that this procedure could be widely applicable to this major class of membrane proteins, as well as to other, more complex, membrane proteins. Indeed, the higher the $m/z$ ratio of the membrane protein complex, the easier its separation from the lower $m/z$ ions arising from the amphipol during ESI-IMS-MS analysis.

Nanodiscs provide an alternate strategy of solubilizing membrane proteins for study by MS.[31] Typically, nanodiscs consist of a lipid bilayer surrounded by a stabilizing scaffold protein into which a membrane protein can be inserted.[4,32,33] Although membrane proteins inside nanodiscs reside in a nativelike environment, the preparation of nanodiscs containing membrane proteins is not straightforward. Several parameters need to be optimized, including the type of lipid and the lipid–protein ratio, which vary for each protein sample. These complex systems have eluded analysis by ESI-MS to date. Insertion of outer membrane proteins into amphipols, by contrast, is relatively straightforward with only the protein/amphipol ratio needing optimization.

As amphipols become more commercially available, the study of membrane proteins in amphipols should become increasingly utilized within the membrane protein field. The additional stability that amphipols offer makes these membrane protein–amphipol complexes highly favorable over traditional methods that use detergent to solubilize the membrane proteins of interest. Since membrane proteins constitute approximately 30% of the proteome and more than 50% of all known drug targets, the study of membrane proteins by high-throughput mass spectrometric techniques will become increasingly important for this challenging field of research.

## AUTHOR INFORMATION

### Corresponding Author

*Phone: 0113 343 7273 (A.E.A.). Fax: 0113 343 7273 (A.E.A.); 0113 343 7486 (S.E.R.). E-mail: a.e.ashcroft@leeds.ac.uk (A.E.A.); s.e.radford@leeds.ac.uk (S.E.R.).

### Notes

The authors declare no competing financial interest.

## ACKNOWLEDGMENTS

We thank Dr. Bethny Morrissey for initiating noncovalent membrane protein mass spectrometry analysis in the Ashcroft and Radford groups and Dr. Charlotte A. Scarff for assistance with the theoretical cross-sectional area calculations. We thank Dr. Alice I. Bartlett, Dr. Gerard H. M. Huysmans, and Dr. David J. Brockwell for helpful discussions and valuable advice. The PagP plasmid was kindly provided by Dr. Russell Bishop (McMaster University). A.C.L was funded by the Biotechnology and Biological Sciences Research Council (BBSRC) with CASE sponsorship from Micromass U.K. Ltd./Waters, Manchester, U.K. (BB/526502/1). L.M.M was funded by the BBSRC (BB/F01614X/1). The Synapt HDMS mass spectrometer was purchased with a research equipment grant from the BBSRC (BB/E012558/1) and the Chirascan CD spectrometer with funding from the Wellcome Trust (094232/Z/10/Z).

## REFERENCES

(1) Seddon, A. M.; Curnow, P.; Booth, P. J. *Biochim. Biophys. Acta, Biomembr.* **2004**, *1666*, 105–117.
(2) Zhou, Y. F.; Lau, F. W.; Nauli, S.; Yang, D.; Bowie, J. U. *Protein Sci.* **2001**, *10*, 378–383.
(3) Garavito, R. M.; Ferguson-Miller, S. *J. Biol. Chem.* **2001**, *276*, 32403–32406.
(4) Popot, J. L. *Annu. Rev. Biochem.* **2010**, *79*, 737–775.
(5) Popot, J. L.; Althoff, T.; Bagnard, D.; Baneres, J. L.; Bazzacco, P.; Billon-Denis, E.; Catoire, L. J.; Champeil, P.; Charvolin, D.; Cocco, M. J.; Cremel, G.; Dahmane, T.; de la Maza, L. M.; Ebel, C.; Gabel, F.; Giusti, F.; Gohon, Y.; Goormaghtigh, E.; Guittet, E.; Kleinschmidt, J. H.; Kuhlbrandt, W.; Le Bon, C.; Martinez, K. L.; Picard, M.; Pucci, B.; Sachs, J. N.; Tribet, C.; van Heijenoort, C.; Wien, F.; Zito, F.; Zoonens, M. *Annu. Rev. Biophys.* **2011**, *40*, 379–408.
(6) Gohon, Y.; Dahmane, T.; Ruigrok, R. W. H.; Schuck, P.; Charvolin, D.; Rappaport, F.; Timmins, P.; Engelman, D. M.; Tribet, C.; Popot, J. L.; Ebel, C. *Biophys. J.* **2008**, *94*, 3523–3537.
(7) Cvetkov, T. L.; Huynh, K. W.; Cohen, M. R.; Moiseenkova-Bell, V. Y. *J. Biol. Chem.* **2011**, *286*, 38168–38176.
(8) Zoonens, M.; Giusti, F.; Zito, F.; Popot, J. L. *Biochemistry* **2007**, *46*, 10392–10404.
(9) Zoonens, M.; Catoire, L. J.; Giusti, F.; Popot, J. L. *Proc. Natl. Acad. Sci. U.S.A.* **2005**, *102*, 8893–8898.
(10) Catoire, L. J.; Zoonens, M.; van Heijenoort, C.; Giusti, F.; Popot, J. L.; Guittet, E. *J. Magn. Reson.* **2009**, *197*, 91–95.
(11) Catoire, L. J.; Damian, M.; Giusti, F.; Martin, A.; van Heijenoort, C.; Popot, J. L.; Guittet, E.; Baneres, J. L. *J. Am. Chem. Soc.* **2010**, *132*, 9049–9057.
(12) Bechara, C.; Bolbach, G.; Bazzaco, P.; Sharma, K. S.; Durand, G.; Popot, J.-L.; Zito, F.; Sagan, S. *Anal. Chem.* **2012**, *84*, 6128–6135.
(13) Huysmans, G. H. M.; Radford, S. E.; Brockwell, D. J.; Baldwin, S. A. *J. Mol. Biol.* **2007**, *373*, 529–540.
(14) Burgess, N. K.; Dao, T. P.; Stanley, A. M.; Fleming, K. G. *J. Biol. Chem.* **2008**, *283*, 26748–26758.
(15) Kramer, R. A.; Zandwijken, D.; Egmond, M. R.; Dekker, N. *Eur. J. Biochem.* **2000**, *267*, 885–893.
(16) Knapman, T. W.; Berryman, J. T.; Campuzano, I.; Harris, S. A.; Ashcroft, A. E. *Int. J. Mass Spectrom.* **2010**, *298*, 17–23.
(17) Smith, D. P.; Knapman, T. W.; Campuzano, I.; Malham, R. W.; Berryman, J. T.; Radford, S. E.; Ashcroft, A. *Eur. J. Mass Spectrom.* **2009**, *15*, 113–130.
(18) Bleiholder, C.; Wyttenbach, T.; Bowers, M. T. *Int. J. Mass Spectrom.* **2011**, *308*, 1–10.
(19) Hagan, C. L.; Silhavy, T. J.; Kahne, D. *Annu. Rev. Biochem.* **2011**, *80*, 189–210.
(20) Brandenburg, K.; Garidel, P.; Schromm, A. B.; Andra, J.; Kramer, A.; Egmond, M.; Wiese, A. *Eur. Biophys. J. Biophys. Lett.* **2005**, *34*, 28–41.
(21) Schnaitman, C. A. *Arch. Biochem. Biophys.* **1973**, *157*, 541–552.
(22) Hagan, C. L.; Kim, S.; Kahne, D. *Science* **2010**, *328*, 890–892.
(23) Kramer, R. A.; Brandenburg, K.; Vandeputte-Rutten, L.; Werkhoven, M.; Gros, P.; Dekker, N.; Egmond, M. R. *Eur. J. Biochem.* **2002**, *269*, 1746–1752.
(24) Bishop, R. E. *Mol. Microbiol.* **2005**, *57*, 900–912.
(25) Khan, M. A.; Neale, C.; Michaux, C.; Pomes, R.; Prive, G. G.; Woody, R. W.; Bishop, R. E. *Biochemistry* **2007**, *46*, 4565–4579.
(26) Cuesta-Seijo, J. A.; Neale, C.; Khan, M. A.; Moktar, J.; Tran, C. D.; Bishop, R. E.; Pomes, R.; Prive, G. G. *Structure* **2010**, *18*, 1210–1219.
(27) Khan, M. A.; Moktar, J.; Mott, P. J.; Bishop, R. E. *Biochemistry* **2010**, *49*, 2368–2379.

(28) Aminlashgari, N.; Hakkarainen, M. *Mass Spectrometry of Polymers—New Techniques*; Springer-Verlag: Berlin, Germany, 2012; Vol. *248*, p 1.
(29) Ruotolo, B. T.; Benesch, J. L. P.; Sandercock, A. M.; Hyung, S. J.; Robinson, C. V. *Nat. Protoc.* **2008**, *3*, 1139−1152.
(30) Barrera, N. P.; Robinson, C. V. *Annu. Rev. Biochem.* **2011**, *80*, 247−271.
(31) Marty, M. T.; Das, A.; Sligar, S. G. *Anal. Bioanal. Chem.* **2012**, *402*, 721−729.
(32) Bayburt, T. H.; Sligar, S. G. *FEBS Lett.* **2010**, *584*, 1721−1727.
(33) Ritchie, T. K.; Grinkova, Y. V.; Bayburt, T. H.; Denisov, I. G.; Zolnerciks, J. K.; Atkins, W. M.; Sligar, S. G. *Methods in Enzymology; Liposomes*; Elsevier Academic Press: San Diego, CA, 2009; Vol. *464*, pp 211−231.
(34) Vandeputte-Rutten, L.; Kramer, R. A.; Kroon, J.; Dekker, N.; Egmond, M. R.; Gros, P. *EMBO J.* **2001**, *20*, 5033−5039.
(35) Ahn, V. E.; Lo, E. I.; Engel, C. K.; Chen, L.; Hwang, P. M.; Kay, L. E.; Bishop, R. E.; Prive, G. G. *EMBO J.* **2004**, *23*, 2931−2941.